Adaptive Predefined-Time Event-Triggered Consensus Tracking Control for Robotic Multi-Agent System

Tengying Yan, Xinliang Zhao, Yuhan Zhang, Yulong Ji, and Ben Niu

***Abstract*—This paper proposes a novel adaptive predefined-time control strategy for the *n*-link robotic multi-agent systems (MASs) to achieve the consensus tracking control. First, unlike existing research on the control problems of a single robotic manipulator system, the consensus tracking control problem of the robotic MASs is studied. Then, in contrast to the finite-time and fixed-time control theories, the controller constructed based on the predefined-time control theory enables the user to define the convergence time of each agent in advance, regardless of the initial state and parameters of the system. The radial basis function neural networks (RBFNNs) are applied to approximate the unknown functions during the controller design process. Only one parameter is updated online, which saves computational costs. Moreover, to deal with the shortage of network resources that may occur when the robotic MASs perform complex tasks, the controllers are constructed by combining the switching threshold event-triggered control (ETC) mechanism to save communication resources. Finally, a simulation example demonstrates the efficacy of the proposed control strategy.**

***Index Terms*—Adaptive control, robotic multi-agent system (MAS), predefined-time control, leader-following consensus, event-triggered control (ETC)**

I. INTRODUCTION

OVER the last two decades, the multi-agent systems (MASs) have become widely prevalent in various fields, including artificial intelligence [1], machine learning [2], automation [3], etc. The MAS is a system formed by the interaction and collaboration of multiple agents. Each agent has a certain degree of autonomy and decision-making ability, and communicates, collaborates, and competes with each other to achieve the goals of the system as a whole. Consensus control is a significant research topic in the field of cooperative control of MASs. Its goal is to create distributed protocols that enable all agents to achieve consensus. This topic has gained increasing interest and has yielded many outstanding research results [4–6]. A new adaptive backstepping finite-time optimal formation controller based on an optimal performance indicator function that contained an exponential power term was constructed for the second-order MASs with unknown nonlinear dynamics in Ref. [7]. Reference [8] proposed an adaptive neural network trajectory tracking control scheme for the n-degree of freedom (DOF) robotic manipulators under parameter variations, unknown functions, and time-varying external disturbances. To guarantee the transient performance of the system, an adaptive fuzzy control strategy was studied for the single-link robotic manipulator with prescribed performance in Ref. [9]. However, the aforementioned studies only tackled the control problem of individual robotic manipulator systems without considering the consensus tracking control problem in robotic MASs. Compared with single agents, MASs offer higher efficiency, resource conservation, and enhanced reliability, making them widely used in practical production. Since leaders only transmit information to a limited number of agents, solving the consensus tracking control problem for robotic MASs poses a significant challenge.

In the domain of consensus control, assessing the control performance of designed protocols often involves the crucial metric of convergence time [10–12]. For example, Ref. [13] devised a distributed adaptive finite-time control protocol, in which all signals in the closed-loop system stayed within defined boundaries and achieved consensus tracking control within a finite-time. In order to address the interplay between unknown model uncertainties and actuator faults, an adaptive finite-time fault-tolerant control scheme was proposed, which leveraged a Lyapunov function to ensure the stability of the closed-loop system and exhibited a practical finite-time state tracking property [14]. Although the finite-time control method enhances the convergence performance of the systems, the convergence time is related to the initial state. Thus, the fixed-time control strategy has garnered extensive research interest. For instance, in the presence of time-varying delay and uncertainties in dynamics, Ref. [15] established a new adaptive fixed-time stability analysis criterion to prove that the closed-loop system with parametric uncertainties was fixed-time stable and all the states could be regulated to zero. Both the finite-time control and fixed-time control theories are advanced control strategies designed to ensure system stability and performance requirements within a predetermined time frame [16–18]. Their applications usually involve areas with high requirements for real-time and predictability.

However, in the realm of finite-time and fixed-time stability, the settling-time function is affected by the initial states and system parameters. Therefore, for the system with determined parameters, the setting time cannot be

Manuscript received: 18 October 2024; revised: 19 December 2024; accepted: 7 January 2025. *(Corresponding author: Tengying Yan.)*

Citation: T. Yan, X. Zhao, Y. Zhang, Y. Ji, and B. Niu, Adaptive predefined-time event-triggered consensus tracking control for robotic multi-agent system, *Int. J. Intell. Control Syst.*, 2025, 30(1), 16–26.

Tengying Yan, Xinliang Zhao, Yuhan Zhang, Yulong Ji, and Ben Niu are with School of Information Science and Engineering, Shandong Normal University, Jinan 250014, China (e-mail: tyingyan778@163.com; xinliangz2022@163.com; zyh9968g@163.com; yuloongee@yeah.net; niubensdnu@163.com).

Digital Object Identifier 10.62678/IJICS202503.10134

predetermined. To address this issue, the predefined-time control method is developed, ensuring that the settling time can be explicitly predetermined without considering initial states and system parameters, which enables this method to be suitable for practical devices. For possible scenarios, including changes in system parameters, such as inertia and damping, as well as the mechanical or dynamic parameters of individual robots, which may vary slightly in multi-robot systems, the predefined-time control method decouples the convergence time from system parameters, thus improving the robustness of the control method to parameter uncertainties. In recent years, this technology has produced many excellent results. Reference [19] presented a lemma aimed at achieving predefined-time stability within the backstepping framework, in which the critical distinctive aspect lied in the capability to predefine the convergence time based on user specifications. Reference [20] proposed a predefined-time fault-tolerant tracking control strategy based on the backstepping method for the high-order strict-feedback nonlinear systems that might experience actuator faults and unknown mismatched disturbances. The utilization of robot manipulators in actual production is progressively expanding. In some cases, it is necessary to calculate the convergence time and convergence accuracy for the robotic MASs. In light of both practical application requirements and theoretical underpinnings, how to design the consensus tracking control scheme for robotic MASs is a challenging and meaningful research topic.

The robotic MASs may suffer from a lack of communication resources when performing complex tasks. In the traditional time-triggered strategy, the control signal is updated regularly at fixed time intervals. This can result in a large number of redundant transmissions after the system stabilizes. Reference [21] studied a fixed threshold event-triggered control (ETC) strategy, in which the measurement error of the control signal was always limited to a constant quantity, irrespective of how the control signal magnitude changed. The fixed threshold ETC strategy lacks flexibility and may not meet the performance requirements of different tasks. The relative threshold ETC strategy may result in significant measurement errors and a sudden jump in the controller signal when the control signal magnitude changes excessively [22]. Therefore, avoiding the disadvantages of the above strategies is very important. Due to the presence of unknown nonlinearities in the robotic MASs, it is a challenge to realize predefined-time consensus tracking control for the robotic MASs. The neural networks can effectively deal with these unknown nonlinearities, because they can learn and adapt to complex nonlinear relationships [23–25]. Therefore, applying neural networks to approximate the unknown functions in the consensus tracking control for the robotic MASs has sparked our research interest.

For the robotic MASs, a new adaptive predefined-time event-triggered consensus tracking control strategy is proposed. The primary highlights of the article are summarized as follows:

(1) Compared with the studies of a single robotic manipulator system [26–28], this paper considers the consensus tracking control problem for the robotic MASs, so that all the agents can track the signal of the leader.

(2) In contrast to the conventional finite-time [29] and fixed-time [30] control approaches, a novel controller constructed in this study ensures that the tracking errors converge within a predefined time specified by the user, regardless of the initial conditions.

(3) The paper implements the switching threshold ETC strategy to develop the controller for each agent, leading to the efficient conservation of communication resources within the system. Additionally, unlike the fixed threshold and relative threshold ETC strategies discussed in previous studies, the switching threshold ETC strategies proposed in this paper offers greater flexibility in adjusting system performance.

II. Preliminary and Problem Establishment

A. Graph Theory

The directed graph can be denoted as $G=(U,N_L)$, where $U=\{u_1,u_2,...,u_k\}$ is the node set and $N_L \subseteq U\times U$ represents the edge set. $e_{ji}=(u_j,u_i)\in N_L$ can be depicted as the edge, implying that the agent i gets information from the agent j. In the directed graph, the adjacency matrix can be denoted as $A=[a_{ij}]\in\mathbb{R}^{k\times k}$. If $e_{ji}=(u_j,u_i)\in N_L$, $a_{ij}>0$. The case of self-loops is usually not considered. Define $D=\text{diag}(d_1, d_2,...,d_k)\in\mathbb{R}^{k\times k}$ as an in-degree matrix containing $d_i=\sum_{j=1}^{N}a_{ij}$. Then, the Laplacian matrix can be denoted by $L=D-A$ in the directed graph G. Additionally, a matrix $B=\text{diag}(b_1,b_2,...,b_k)\in\mathbb{R}^{k\times k}$ is defined, b_i is the weight between the leader and the agent i.

B. Problem Establishment

The robotic MASs consist of N ($N\geqslant 2$) followers (signed in order, 1 to N) and a leader (signed d). Then, the plant dynamics of the i-th ($i=1,2,...,N$) n-link robotic manipulator system is

$$M_i(q_i)\ddot{q}_i+C_i(q_i,\dot{q}_i)\dot{q}_i+G_i(q_i)+f_{\text{dis}}(t)=\tau_i \tag{1}$$

where q_i, $\dot{q}_i$, and $\ddot{q}_i\in\mathbb{R}^n$ represent the angle, the angular velocity, and the angular acceleration of the system, which are all system states. $M_i(q_i)$, $C_i(q_i,\dot{q}_i)\in\mathbb{R}^{n\times n}$, and $G_i(q_i)\in\mathbb{R}^n$ are the inertia matrix, the centrifugal-Coriolis matrix, and the gravity term, respectively. $f_{\text{dis}}(t)\in\mathbb{R}^n$ denotes the disturbance term. $\tau_i\in\mathbb{R}^n$ represents the control term, $\tau_i=[\tau_{i,1},\tau_{i,2}]^{\text{T}}$, where $\tau_{i,j}$, $j=1,2$ denotes the control input at link j of the i-th robot. In order to facilitate subsequent design, $M_i(q_i)$, $C_i(q_i,\dot{q}_i)$, $G_i(q_i)$, and $f_{\text{dis}}(t)$ are simplified to M_i, C_i, G_i, and f_{dis}.

By introducing the state variables $x_{i,1}=q_i$ and $x_{i,2}=\dot{q}_i$, we convert Eq. (1) into the following form of the strict-feedback system

$$\begin{cases}\dot{x}_{i,1}=x_{i,2},\\ \dot{x}_{i,2}=M_i^{-1}(\tau_i-C_ix_{i,2}-G_i-f_{\text{dis}}),\\ y_i=x_{i,1}\end{cases} \tag{2}$$

where $x_{i,j}=[x_{i,j_1},x_{i,j_2},...,x_{i,j_n}]^{\text{T}}\in\mathbb{R}^{2\times n}$, $j=1,2$ represents the system state. $\tau_i\in\mathbb{R}^n$ and $y_i\in\mathbb{R}^n$ denote the control input and the output of the i-th system, respectively. Additionally, the leader dynamic model is

$$\begin{cases}\dot{x}_{\text{d}}=f_{\text{d}}(x_{\text{d}},t),\\ y_{\text{d}}=x_{\text{d}}\end{cases} \tag{3}$$

where $x_{\rm d} \in \mathbb{R}^n$ denotes the state of leader, $f_{\rm d}(x_{\rm d}, t)$ represents a piecewise continuous function with respect to t that satisfies the local Lipschitz condition, and $y_{\rm d} \in \mathbb{R}^n$ is the leader's output.

C. Useful Assumption and Lemma

Assumption 1 For a continuous function $f(\cdot)$ and a constant $X_{\rm d} > 0$, the following inequalities hold for all $t \geqslant 0$: $|f_{\rm d}(x_{\rm d}, t)| \leqslant f(x_{\rm d})$ and $|x_{\rm d}(t)| \leqslant X_{\rm d}$.

Lemma 1 [31] Define $z_1 = (z_{1,1}, z_{2,1}, ..., z_{N,1})^{\rm T}$, $y = (y_1, y_2, ..., y_N)^{\rm T}$, and $\bar{y}_{\rm d} = (y_{\rm d}, y_{\rm d}, ..., y_{\rm d})^{\rm T} \in \mathbb{R}^N$, we can obtain

$$\|y - \bar{y}_{\rm d}\| \leqslant \|z_1\| / \sigma(L+B) \tag{4}$$

with $\sigma(L+B)$ being the minimum singular value of $L+B$.

Lemma 2 [32] For any vectors p and $q \in \mathbb{R}^2$, one has

$$pq \leqslant \frac{l^a}{a}|p|^a + \frac{1}{bl^b}|q|^b \tag{5}$$

where $l > 0$, $a > 1$, $b > 1$, and $(a-1)(b-1) = 1$.

Lemma 3 [33] Let $\mu_1, \mu_2, ..., \mu_Q \geqslant 0$, $0 < c \leqslant 1$, and $d > 1$, one has

$$\sum_{i=1}^{Q} \mu_i^c \geqslant \left(\sum_{i=1}^{Q} \mu_i\right)^c \tag{6}$$

$$\sum_{i=1}^{Q} \mu_i^d \geqslant Q^{1-d}\left(\sum_{i=1}^{Q} \mu_i\right)^d \tag{7}$$

Lemma 4 [34] For $\forall \lambda \in \mathbb{R}$ and $\beta > 0$, we can obtain

$$0 \leqslant |\lambda| - \lambda \tanh\left(\frac{\lambda}{\beta}\right) \leqslant 0.2785\beta \tag{8}$$

Lemma 5 [35] Any continuous unknown function can be approximated in general for the RBFNNs. The unknown function $g(\vartheta)$ can be approximated by

$$g(\vartheta) = \psi^{*{\rm T}} S(\vartheta) + \delta(\vartheta), \ \forall \vartheta \in \Omega_\vartheta \subset \mathbb{R}^m \tag{9}$$

where $\delta(\vartheta)$ is the approximation error satisfying $|\delta(\vartheta)| \leqslant \bar{\delta}$ with $\bar{\delta}$ being a given precise value. $S(\vartheta) = [S_1(\vartheta), S_2(\vartheta), ..., S_q(\vartheta)]^{\rm T}$ is the basis function vector and $q > 1$ is node number. Ω_ϑ is a compact set. $S_i(\vartheta)$ is defined as the following Gaussian form

$$S_i(\vartheta) = \exp\left[-\frac{(\vartheta - u_i)^{\rm T}(\vartheta - u_i)}{\zeta^2}\right], \ i = 1, 2, ..., q \tag{10}$$

where $u_i = [u_{i1}, u_{i2}, ..., u_{im}]^{\rm T}$ and ζ represent the center and the width of $S_i(\vartheta)$, respectively. Furthermore, $\psi^* = [\psi_1, \psi_2, ..., \psi_q]^{\rm T}$ is an ideal weight vector defined as

$$\psi^* = \arg\min_{\psi \in \mathbb{R}^q} \left\{\sup_{\vartheta \in \Omega_\vartheta} \left|g(\vartheta) - \psi^{\rm T} S(\vartheta)\right|\right\} \tag{11}$$

Lemma 6 [36] Suppose that $\varphi(\bar{\gamma}_r) = [\varphi_1(\bar{\gamma}_r), \varphi_2(\bar{\gamma}_r), ..., \varphi_q(\bar{\gamma}_r)]^{\rm T}$ is the basis function vector of RBFNNs, where $\bar{\gamma}_r = [\gamma_1, \gamma_2, ..., \gamma_r]^{\rm T}$. For any integer $0 < m \leqslant n$, we further obtain

$$\|\varphi(\bar{\gamma}_n)\|^2 \leqslant \|\varphi(\bar{\gamma}_m)\|^2 \tag{12}$$

Lemma 7 [37] For a system dynamic $\dot{\sigma}(t) = F(t, \sigma)$ and $\sigma(0) = \sigma_0$, where $\sigma \in \mathbb{R}^n$ and $F(\cdot): \mathbb{R}^+ \times \mathbb{R}^n \to \mathbb{R}^n$, the equilibrium point $x = 0$ of the system is semiglobally uniformly predefined-time-bounded (SGUPTB) stable, if there is a positive-definite function and continuously differentiable $V(x)$ satisfying

$$\dot{V}(x) \leqslant -\frac{\gamma}{T_\rho}(aV^p(x) + bV^q(x))^k - cV(x) + \delta_\rho \tag{13}$$

where a, b, p, q, and k are positive constants. The constant T_ρ is chosen, such that $T_\rho \geqslant T_o > 0$ (T_o denotes the physically possible time range) and is referred to as the predefined time. $c > 0$ and $\delta_\rho > 0$ are bounded constants satisfying, $0 < pk < 1$, $qk > 1$, and

$$\gamma = \frac{\Gamma(m_1)\Gamma(m_2)}{a^k \Gamma(k)(q-p)}\left(\frac{a}{b}\right)^{m_1} \tag{14}$$

where $m_1 = [(1-pk)/(q-p)]$ and $m_2 = [(qk-1)/(q-p)]$. $\Gamma(t)$ is the Gamma function defined as $\Gamma(t) = \int_0^{+\infty} {\rm e}^{-\tau}\tau^{t-1}{\rm d}\tau$.

III. Main Result

In this section, a predefined-time controller is designed for each agent by using the backstepping method, RBFNNs theory, and adaptive strategy. Some symbols need to be stated. For $\chi \in \mathbb{R}^n$, $\|\chi\|$ is the Euclidean norm. Define $\theta_i = \max\|\psi_{i,j}\|^2$, $\psi_{i,j} = {\rm diag}(\psi_{i,j_k}^{*{\rm T}})$, $j = 1, 2$, and $k = 1, 2, ..., n$. $\psi_{i,j_k}^{*{\rm T}}$ and $S_{i,j}(\cdot)$ denote the ideal weight vector and the basis function vector of RBFNNs, respectively. Let ${\rm sgn}^\alpha(x) = (|x_1|^\alpha {\rm sgn}(x_1), |x_2|^\alpha {\rm sgn}(x_2), ..., |x_n|^\alpha {\rm sgn}(x_n))^{\rm T}$, where $\alpha > 0$ and ${\rm sgn}(x_i)$ is the sign function defined as

$${\rm sgn}(x_i) = \begin{cases} 1, \text{ if } x_i > 0; \\ 0, \text{ if } x_i = 0; \\ -1, \text{ if } x_i < 0 \end{cases} \tag{15}$$

Then, the consensus tracking control strategy is obtained by using the following coordinate transformation

$$\begin{cases} z_{i,1} = \sum_{j=1}^{N} a_{ij}(y_i - y_j) + b_i(y_i - y_{\rm d}), \\ z_{i,2} = x_{i,2} - \alpha_{i,1} \end{cases} \tag{16}$$

where $i = 1, 2, ..., N$, a_{ij} and b_i are already defined in the graph theory, and $\alpha_{i,1}$ is the virtual control signal for the i-th agent.

Construct the following Lyapunov function

$$V(t) = V_{i,1}(t) + V_{i,2}(t) + V_{i,3}(t) \tag{17}$$

where $V_{i,1}(t) = (z_{i,1}^{\rm T}(t) z_{i,1}(t))/2$, $V_{i,2}(t) = (z_{i,2}^{\rm T}(t) z_{i,2}(t))/2$, and $V_{i,3}(t) = \tilde{\theta}_i^2(t)/2$. To facilitate subsequent derivation, time t is omitted.

It follows from Eq. (16) that

$$\dot{z}_{i,1} = (d_i + b_i)x_{i,2} - b_i f_{\rm d}(x_{\rm d}, t) - \sum_{j=1}^{N} a_{ij} x_{j,2} \tag{18}$$

Differentiating $V_{i,1}$ gives

$$\dot{V}_{i,1} = z_{i,1}^{\rm T}\left[(d_i + b_i)(z_{i,2} + \alpha_{i,1}) - b_i f_{\rm d}(x_{\rm d}, t) - \sum_{j=1}^{N} a_{ij} x_{j,2}\right] \tag{19}$$

Using Assumption 1 and Lemma 4, there is a designed $\varepsilon > 0$ satisfying Formula (20).

$$-b_i z_{i,1}^{\mathrm{T}} f_{\mathrm{d}}(x_{\mathrm{d}}, t) \leqslant \left| b_i z_{i,1}^{\mathrm{T}} f(x_{\mathrm{d}}) \right| \leqslant b_i z_{i,1}^{\mathrm{T}} f(x_{\mathrm{d}}) \tanh\left(\frac{b_i z_{i,1}^{\mathrm{T}} f(x_{\mathrm{d}})}{\varepsilon} \right) + 0.2785\varepsilon \tag{20}$$

Then, substituting Formula (20) into Eq. (19) yields

$$\dot{V}_{i,1} \leqslant z_{i,1}^{\mathrm{T}} [(d_i + b_i)(z_{i,2} + \alpha_{i,1}) + g_{i,1}(\upsilon_i)] + 0.2785\varepsilon \tag{21}$$

with

$$g_{i,1}(\upsilon_i) = -\sum_{j=1}^{N} a_{ij} x_{j,2} + b_i f(x_{\mathrm{d}}) \tanh\left(\frac{b_i z_{i,1}^{\mathrm{T}} f(x_{\mathrm{d}})}{\varepsilon} \right) \tag{22}$$

where $g_{i,1}(\upsilon_i) = [g_{i,1_1}(\upsilon_{i_1}), g_{i,1_2}(\upsilon_{i_2}), \ldots, g_{i,1_n}(\upsilon_{i_n})]^{\mathrm{T}}$ and $\upsilon_i = [x_i, x_j, x_{\mathrm{d}}]^{\mathrm{T}}$.

Equation (23) holds by using Lemma 5

$$g_{i,1_k}(\upsilon_{i_k}) = \psi_{i,1_k}^{*\mathrm{T}} S_{i,1}(\upsilon_{i_k}) + \delta_{i,1_k}(\upsilon_{i_k}) \tag{23}$$

where $k = 1, 2, \ldots, n$ and $\upsilon_{i_k} = [x_{i_k}, x_{j_k}, x_{\mathrm{d}_k}]^{\mathrm{T}}$, $x_{i_k} = [x_{i,1_k}, x_{i,2_k}]^{\mathrm{T}}$ and x_{d_k} denotes the k-th element of x_{d}. $|\delta_{i,1_k}(\upsilon_{i_k})| \leqslant \bar{\delta}$ with $\bar{\delta}$ being a given value.

From Lemma 6, one has

$$g_{i,1_k}(\upsilon_{i_k}) \leqslant \psi_{i,1_k}^{*\mathrm{T}} S_{i,1}(\upsilon_{i,1_k}) + \bar{\delta} \tag{24}$$

where $\upsilon_{i,1_k} = [x_{i,1_k}, x_{j,1_k}, x_{\mathrm{d}_k}]^{\mathrm{T}}$.

Based on Formula (24) and the definitions of θ_i and $g_{i,1}$, we have

$$z_{i,1}^{\mathrm{T}} g_{i,1} \leqslant \frac{z_{i,1}^{\mathrm{T}} z_{i,1} \psi_{i,1}^{\mathrm{T}} \psi_{i,1} S_{i,1}^{\mathrm{T}}(\upsilon_{i,1}) S_{i,1}(\upsilon_{i,1})}{2 l_{i,1}^2} \leqslant \frac{\theta_i z_{i,1}^{\mathrm{T}} z_{i,1} S_{i,1}^{\mathrm{T}}(\upsilon_{i,1}) S_{i,1}(\upsilon_{i,1})}{2 l_{i,1}^2} + \frac{l_{i,1}^2}{2} + \frac{z_{i,1}^{\mathrm{T}} z_{i,1}}{2} + \frac{n\bar{\delta}^2}{2} \tag{25}$$

where $\upsilon_{i,1} = [x_{i,1_1}, x_{i,1_2}, \ldots, x_{i,1_n}, x_{j,1_1}, x_{j,1_2}, \ldots, x_{j,1_n}, x_{\mathrm{d}_1}, x_{\mathrm{d}_2}, \ldots, x_{\mathrm{d}_n}]^{\mathrm{T}}$ and $l_{i,1} > 0$ is a given real number. $S_{i,1}(\upsilon_i)$ is abbreviated as $S_{i,1}$.

Substituting Formula (25) into Formula (21) gives

$$\dot{V}_{i,1} \leqslant z_{i,1}^{\mathrm{T}} [(d_i + b_i) z_{i,2} + (d_i + b_i)\alpha_{i,1}] + \frac{\theta_i z_{i,1}^{\mathrm{T}} z_{i,1} S_{i,1}^{\mathrm{T}} S_{i,1}}{2 l_{i,1}^2} + \frac{l_{i,1}^2}{2} + \frac{z_{i,1}^{\mathrm{T}} z_{i,1}}{2} + \frac{n\bar{\delta}^2}{2} + 0.2785\varepsilon \tag{26}$$

The virtual control signal $\alpha_{i,1}$ is designed as

$$\alpha_{i,1} = \frac{1}{d_i + b_i} \left[-\frac{1+\sigma}{2} z_{i,1} - \frac{\gamma}{\sqrt{2} T_\rho} \left(2^{-\frac{\alpha}{2}} \frac{z_{i,1}}{z_{i,1}^{\mathrm{T}} z_{i,1}} \varpi_{i,1} + 2^{-\frac{\beta}{2}} \frac{z_{i,1}}{z_{i,1}^{\mathrm{T}} z_{i,1}} (z_{i,1}^{\mathrm{T}} z_{i,1})^{\frac{1+\beta}{2}} \right) - \frac{\hat{\theta}_i z_{i,1} S_{i,1}^{\mathrm{T}} S_{i,1}}{2 l_{i,1}^2} \right] \tag{27}$$

with T_ρ being the predefined time, $\sigma > 0$ and $\varpi_{i,1}$ being designed as

$$\varpi_{i,1} = \begin{cases} (z_{i,1}^{\mathrm{T}} z_{i,1})^{\frac{1+\alpha}{2}}, & z_{i,1}^{\mathrm{T}} z_{i,1} \geqslant \lambda_{10}; \\ \sum_{j=1}^{2} a_j (z_{i,1}^{\mathrm{T}} z_{i,1})^j (\lambda_{10}^2)^{-j+\frac{1+\alpha}{2}}, & z_{i,1}^{\mathrm{T}} z_{i,1} < \lambda_{10} \end{cases} \tag{28}$$

where $\lambda_{10} > 0$, a_1 and a_2 are given as

$$\begin{bmatrix} 1 & 1 \\ 1 & 2 \end{bmatrix} \begin{bmatrix} a_1 \\ a_2 \end{bmatrix} = \begin{bmatrix} b_1 \\ b_2 \end{bmatrix} \tag{29}$$

where $b_1 = 1$ and $b_2 = (1+\alpha)/2$.

Substituting Eq. (27) into Formula (26) obtains

$$V_{i,1} \leqslant -\frac{\gamma}{\sqrt{2} T_\rho} \left[2^{-\frac{\alpha}{2}} \varpi_{i,1} + 2^{-\frac{\beta}{2}} (z_{i,1}^{\mathrm{T}} z_{i,1})^{\frac{1+\beta}{2}} \right] + \frac{\tilde{\theta}_i z_{i,1}^{\mathrm{T}} z_{i,1} S_{i,1}^{\mathrm{T}} S_{i,1}}{2 l_{i,1}^2} - \frac{\sigma}{2} z_{i,1}^{\mathrm{T}} z_{i,1} + (d_i + b_i) z_{i,1}^{\mathrm{T}} z_{i,2} + \varDelta_1 \tag{30}$$

where $\varDelta_1 = l_{i,1}^2/2 + n\bar{\delta}^2/2 + 0.2785\varepsilon$.

For the first items of Formula (30) and Eq. (28), we can get the two cases below.

Case 1: If $z_{i,1}^{\mathrm{T}} z_{i,1} \geqslant \lambda_{10}$, then

$$-\frac{\gamma}{\sqrt{2} T_\rho} \left[2^{-\frac{\alpha}{2}} \varpi_{i,1} + 2^{-\frac{\beta}{2}} (z_{i,1}^{\mathrm{T}} z_{i,1})^{\frac{1+\beta}{2}} \right] = -\frac{\gamma}{T_\rho} \left[\left(\frac{z_{i,1}^{\mathrm{T}} z_{i,1}}{2} \right)^{\frac{1+\alpha}{2}} + \left(\frac{z_{i,1}^{\mathrm{T}} z_{i,1}}{2} \right)^{\frac{1+\beta}{2}} \right] = -\frac{\gamma}{T_\rho} V_{i,1}^{\frac{1+\alpha}{2}} - \frac{\gamma}{T_\rho} V_{i,1}^{\frac{1+\beta}{2}} \tag{31}$$

Thus, substituting Eq. (31) into Formula (30), one gets

$$\dot{V}_{i,1} \leqslant -\sigma V_{i,1} - \frac{\gamma}{T_\rho} V_{i,1}^{\frac{1+\alpha}{2}} - \frac{\gamma}{T_\rho} V_{i,1}^{\frac{1+\beta}{2}} + (d_i + b_i) z_{i,1}^{\mathrm{T}} z_{i,2} + \frac{\tilde{\theta}_i z_{i,1}^{\mathrm{T}} z_{i,1} S_{i,1}^{\mathrm{T}} S_{i,1}}{2 l_{i,1}^2} + \varDelta_1 \tag{32}$$

Case 2: If $z_{i,1}^{\mathrm{T}} z_{i,1} < \lambda_{10}$, then

$$-\frac{\gamma}{\sqrt{2} T_\rho} \left[2^{-\frac{\alpha}{2}} \varpi_{i,1} + 2^{-\frac{\beta}{2}} (z_{i,1}^{\mathrm{T}} z_{i,1})^{\frac{1+\beta}{2}} \right] = -\frac{\gamma}{T_\rho} V_{i,1}^{\frac{1+\alpha}{2}} - \frac{\gamma}{T_\rho} V_{i,1}^{\frac{1+\beta}{2}} + \frac{\gamma}{T_\rho} \left[\left(\frac{z_{i,1}^{\mathrm{T}} z_{i,1}}{2} \right)^{\frac{1+\alpha}{2}} - \sum_{j=1}^{2} a_j (z_{i,1}^{\mathrm{T}} z_{i,1})^j (\lambda_{10}^2)^{-j+\frac{1+\alpha}{2}} \right] \tag{33}$$

Similarly to Formula (32), one obtains

$$\dot{V}_{i,1} \leqslant -\sigma V_{i,1} - \frac{\gamma}{T_\rho} V_{i,1}^{\frac{1+\alpha}{2}} - \frac{\gamma}{T_\rho} V_{i,1}^{\frac{1+\beta}{2}} + (d_i + b_i) z_{i,1}^{\mathrm{T}} z_{i,2} + \frac{\tilde{\theta}_i z_{i,1}^{\mathrm{T}} z_{i,1} S_{i,1}^{\mathrm{T}} S_{i,1}}{2 l_{i,1}^2} + \frac{\gamma}{T_\rho} \left[\left(\frac{z_{i,1}^{\mathrm{T}} z_{i,1}}{2} \right)^{\frac{1+\alpha}{2}} - \sum_{j=1}^{2} a_j (z_{i,1}^{\mathrm{T}} z_{i,1})^j (\lambda_{10}^2)^{-j+\frac{1+\alpha}{2}} \right] + \varDelta_1 \tag{34}$$

Remark 1 Let $\varpi_{i,1} = (z_{i,1}^{\mathrm{T}} z_{i,1})^{\frac{1+\alpha}{2}}$, $\varTheta_{i,1} = (z_{i,1}/(z_{i,1}^{\mathrm{T}} z_{i,1}))\varpi_{i,1}$, then $\dot{\varTheta}_{i,1} = \alpha (z_{i,1}^{\mathrm{T}} z_{i,1})^{\frac{\alpha-1}{2}} \dot{z}_{i,1}$. It is easy to get that $\lim_{z_{i,1}^{\mathrm{T}} z_{i,1} \to 0} \dot{\varTheta}_{i,1}$ does not exist, which creates a singularity problem. By setting $\varpi_{i,1}$ to Eq. (28), we can obtain

$$\dot{\varTheta}_{i,1} = \begin{cases} \alpha (z_{i,1}^{\mathrm{T}} z_{i,1} t)^{\frac{\alpha-1}{2}} \dot{z}_{i,1}, \ z_{i,1}^{\mathrm{T}} z_{i,1} \geqslant \lambda_{10}; \\ \eta(z_{i,1} t) \dot{z}_{i,1}, \ z_{i,1}^{\mathrm{T}} z_{i,1} < \lambda_{10}, \end{cases}$$

where $\eta(z_{i,1}) = a_1 (\lambda_{10}^2)^{\frac{\alpha-1}{2}} + 3 a_2 z_{i,1}^{\mathrm{T}} z_{i,1} (\lambda_{10}^2)^{\frac{\alpha-3}{2}}$. It is easy to conclude that $\lim_{z_{i,1}^{\mathrm{T}} z_{i,1} \to \lambda_{10}} \eta(z_{i,1}) = \alpha (\lambda_{10}^2)^{\frac{\alpha-1}{2}}$ and $\lim_{z_{i,1}^{\mathrm{T}} z_{i,1} \to 0} \eta(z_{i,1}) = a_1 (\lambda_{10}^2)^{\frac{\alpha-1}{2}}$. Thus, the singularity problem of $\dot{\alpha}_{i,1}$ is avoided and its continuity is ensured. If $z_{i,1}^{\mathrm{T}} z_{i,1} < \lambda_{10}$, there is an additional item in Formula (34) compared with Formula (32), which can be regarded as a small incremental change in the constant term $\varDelta_1$. For ease of discussion, only the case of $z_{i,1}^{\mathrm{T}} z_{i,1} \geqslant \lambda_{10}$ is considered in the following analyses.

Next, it follows for $V_{i,2}$ from Eq. (17) that

$$\dot{V}_{i,2} = z_{i,2}^{\mathrm{T}} \dot{z}_{i,2} = z_{i,2}^{\mathrm{T}} (\dot{x}_{i,2} - \dot{\alpha}_{i,1}) = z_{i,2}^{\mathrm{T}} [M_i^{-1} \tau_i + g_{i,2}(\upsilon_i)] \tag{35}$$

with

$$g_{i,2}(\upsilon_i) = M_i^{-1} (-C_i x_{i,2} - G_i - f_{\mathrm{dis}}) - \dot{\alpha}_{i,1} \tag{36}$$

Similarly to Eq. (23), we can obtain

$$g_{i,2_k}(\upsilon_{i_k}) = \psi_{i,2_k}^{*\mathrm{T}} S_{i,2}(\upsilon_{i_k}) + \delta_{i,2_k}(\upsilon_{i_k}) \tag{37}$$

where $|\delta_{i,2_k}(\upsilon_{i_k})| \leqslant \bar{\delta}$.

By the Young's inequality, one has

$$z_{i,2} g_{i,2}(\upsilon_i) \leqslant \frac{\theta_i z_{i,2}^{\mathrm{T}} z_{i,2} S_{i,2}^{\mathrm{T}} S_{i,2}}{2 l_{i,2}^2} + \frac{l_{i,2}^2}{2} + \frac{z_{i,2}^{\mathrm{T}} z_{i,2}}{2} + \frac{n \bar{\delta}^2}{2} \tag{38}$$

where $l_{i,2} > 0$.

Then, Eq. (35) can be rewritten as

$$\dot{V}_{i,2} = z_{i,2}^{\mathrm{T}} M_i^{-1} \tau_i + \frac{\theta_i z_{i,2}^{\mathrm{T}} z_{i,2} S_{i,2}^{\mathrm{T}} S_{i,2}}{2 l_{i,2}^2} + \frac{l_{i,2}^2}{2} + \frac{z_{i,2}^{\mathrm{T}} z_{i,2}}{2} + \frac{n \bar{\delta}^2}{2} \tag{39}$$

To balance the requirements of states monitoring and system performance, the switching threshold ETC mechanism is designed as

$$\begin{cases} \omega_i = -(1+\rho) \left[\alpha_{i,2} \tanh\left(\frac{z_{i,2}^{\mathrm{T}} M_i^{-1} \alpha_{i,2}}{\varepsilon} \right) + \bar{n} \tanh\left(\frac{z_{i,2}^{\mathrm{T}} M_i^{-1} \bar{n}}{\varepsilon} \right) \right], \\ \tau_i(t) = \omega_i(t_k), \ \forall t \in [t_k, t_{k+1}) \end{cases} \tag{40}$$

$$t_{k+1} = \begin{cases} \inf\{ t \in \mathbb{R} \,|\, |e_i(t)| \geqslant \rho |\tau_i(t)| + n_1 \}, \ |\tau_i(t)| < D; \\ \inf\{ t \in \mathbb{R} \,|\, |e_i(t)| \geqslant n_2 \}, \ |\tau_i(t)| \geqslant D \end{cases} \tag{41}$$

where $e_i(t) = \omega_i(t) - \tau_i(t)$. Meanwhile, t_k, $k \in \mathbb{Z}^+$, $0 < \rho < 1$, $\widehat{n} = \max\{n_1, n_2\}$, $\bar{n} > \widehat{n}/(1-\rho)$, n_1, n_2, D, and $\varepsilon > 0$ are all design parameters.

From Eq. (41), we have

$$|\omega_i(t) - \tau_i(t)| \leqslant \rho |\tau_i(t)| + \widehat{n} \tag{42}$$

Define $\delta_1(t)$ and $\delta_2(t)$ as the continuous time-varying parameters satisfying $|\delta_1(t)| < 1$, $|\delta_2(t)| < 1$, $\delta_1(t_k) = \delta_2(t_k) = 0$, and $\delta_1(t_{k+1}) = \delta_2(t_{k+1}) = \pm 1$ for $\forall t \in [t_k, t_{k+1})$.

With the help of Formula (42), the following equations hold.

$$\omega_i - \tau_i = \delta_1 \rho \tau_i(t) + \delta_2 \widehat{n} \tag{43}$$

$$\tau_i(t) = \frac{\omega_i(t) - \delta_2 \widehat{n}}{1 + \delta_1 \rho} \tag{44}$$

where $\delta_1(t)$ and $\delta_2(t)$ are abbreviated to δ_1 and δ_2, respectively.

From Lemma 4 and Formulas (40)–(44), one has

$$\begin{aligned} z_{i,2}^{\mathrm{T}} M_i^{-1} \tau_i = & \frac{-z_{i,2}^{\mathrm{T}} M_i^{-1} (1+\rho)}{1 + \delta_1 \rho} \left[\alpha_{i,2} \tanh\left(\frac{z_{i,2}^{\mathrm{T}} M_i^{-1} \alpha_{i,2}}{\varepsilon} \right) + \bar{n} \tanh\left(\frac{z_{i,2}^{\mathrm{T}} M_i^{-1} \bar{n}}{\varepsilon} \right) \right] - \frac{z_{i,2}^{\mathrm{T}} M_i^{-1} \widehat{n} \delta_2}{1 + \delta_1 \rho} \leqslant \\ & - z_{i,2}^{\mathrm{T}} M_i^{-1} \alpha_{i,2} \tanh\left(\frac{z_{i,2}^{\mathrm{T}} M_i^{-1} \alpha_{i,2}}{\varepsilon} \right) - z_{i,2}^{\mathrm{T}} M_i^{-1} \bar{n} \tanh\left(\frac{z_{i,2}^{\mathrm{T}} M_i^{-1} \bar{n}}{\varepsilon} \right) + \left| \frac{z_{i,2}^{\mathrm{T}} M_i^{-1} \widehat{n} \delta_2}{1 + \delta_1 \rho} \right| \leqslant \\ & - \left| z_{i,2}^{\mathrm{T}} M_i^{-1} \alpha_{i,2} \right| - \left| z_{i,2}^{\mathrm{T}} M_i^{-1} \widehat{n} \right| + 0.557\varepsilon + \left| \frac{z_{i,2}^{\mathrm{T}} M_i^{-1} \widehat{n}}{1 + \delta_1 \rho} \right| \leqslant \\ & z_{i,2}^{\mathrm{T}} M_i^{-1} \alpha_{i,2} + 0.557\varepsilon \end{aligned} \tag{45}$$

The virtual controller $\alpha_{i,2}$ is given as

$$\alpha_{i,2} = -\frac{1}{2} M_i z_{i,2} - (d_i + b_i) M_i z_{i,1} - \frac{\sigma}{2} M_i z_{i,2} - \frac{\gamma}{\sqrt{2} T_\rho} M_i \left[2^{-\frac{\alpha}{2}} \frac{z_{i,2}}{z_{i,2}^{\mathrm{T}} z_{i,2}} \varpi_{i,2} + 2^{-\frac{\beta}{2}} \frac{z_{i,2}}{z_{i,2}^{\mathrm{T}} z_{i,2}} (z_{i,2}^{\mathrm{T}} z_{i,2})^{\frac{1+\beta}{2}} \right] - \frac{\hat{\theta}_i M_i z_{i,2} S_{i,2}^{\mathrm{T}} S_{i,2}}{2 l_{i,2}^2} \tag{46}$$

with $\varpi_{i,2}$ being designed as

$$\varpi_{i,2}=\begin{cases}(z_{i,2}^{\mathrm{T}}z_{i,2})^{\frac{1+\alpha}{2}},\ z_{i,2}^{\mathrm{T}}z_{i,2}\geqslant\lambda_{20};\\ \sum_{j=1}^{2}a_j(z_{i,2}^{\mathrm{T}}z_{i,2})^{j}(\lambda_{20}^2)^{-j+\frac{1+\alpha}{2}},\ z_{i,2}^{\mathrm{T}}z_{i,2}<\lambda_{20}\end{cases} \tag{47}$$

where $\lambda_{20}>0$.

For the fourth item of Eq. (46), one has

$$\begin{aligned}&-\frac{\gamma}{\sqrt{2}T_\rho}z_{i,2}^{\mathrm{T}}\left[2^{-\frac{\alpha}{2}}\frac{z_{i,2}}{z_{i,2}^{\mathrm{T}}z_{i,2}}\varpi_{i,2}+2^{-\frac{\beta}{2}}\frac{z_{i,2}}{z_{i,2}^{\mathrm{T}}z_{i,2}}(z_{i,2}^{\mathrm{T}}z_{i,2})^{\frac{1+\beta}{2}}\right]=\\&-\frac{\gamma}{T_\rho}\left[\left(\frac{z_{i,2}^{\mathrm{T}}z_{i,2}}{2}\right)^{\frac{1+\alpha}{2}}+\left(\frac{z_{i,2}^{\mathrm{T}}z_{i,2}}{2}\right)^{\frac{1+\beta}{2}}\right]=\\&-\frac{\gamma}{T_\rho}V_{i,2}^{\frac{1+\alpha}{2}}-\frac{\gamma}{T_\rho}V_{i,2}^{\frac{1+\beta}{2}}\end{aligned} \tag{48}$$

Substituting Formulas (45)–(48) into Eq. (39), we have

$$\begin{aligned}\dot V_{i,2}=&-(d_i+b_i)z_{i,2}^{\mathrm{T}}z_{i,2}-\sigma V_{i,2}-\frac{\gamma}{T_\rho}V_{i,2}^{\frac{1+\alpha}{2}}-\\&\frac{\gamma}{T_\rho}V_{i,2}^{\frac{1+\beta}{2}}+\frac{\tilde\theta_i z_{i,2}^{\mathrm{T}}z_{i,2}S_{i,2}^{\mathrm{T}}S_{i,2}}{2l_{i,2}^2}+\varDelta_2\end{aligned} \tag{49}$$

where $\varDelta_2=l_{i,2}^2/2+n\bar\delta^2/2+0.557\varepsilon$. $\tilde\theta_i=\theta_i-\hat\theta_i$ is the estimated error of θ_i, $\hat\theta_i$ is the estimated value of θ_i.

Then, for function $V_{i,3}(t)$, we can obtain

$$\dot V_{i,3}=\tilde\theta_i\dot{\tilde\theta}_i=-\tilde\theta_i\dot{\hat\theta}_i \tag{50}$$

The parameter adaptive law $\dot{\hat\theta}_i$ is given as

$$\begin{aligned}\dot{\hat\theta}_i=&\frac{z_{i,1}^{\mathrm{T}}z_{i,1}S_{i,1}^{\mathrm{T}}S_{i,1}}{2l_{i,1}^2}+\frac{z_{i,2}^{\mathrm{T}}z_{i,2}S_{i,2}^{\mathrm{T}}S_{i,2}}{2l_{i,2}^2}-\hat\theta_i-\\&2^{\frac{1+\alpha}{2}}\frac{\gamma}{T_\rho}\mathrm{sgn}^{\alpha}(\hat\theta_i)-2^{\frac{1+\beta}{2}}\frac{\gamma}{T_\rho}\mathrm{sgn}^{\beta}(\hat\theta_i)\end{aligned} \tag{51}$$

Combining Eqs. (50) and (51) and the Young's inequality, one gets

$$\tilde\theta_i\hat\theta_i=\tilde\theta_i\theta_i-\tilde\theta_i^2=\frac12\theta_i^2-\frac12\tilde\theta_i^2 \tag{52}$$

Substituting Eqs. (51) and (52) into Eq. (50) obtains

$$\begin{aligned}\dot V_{i,3}=&-\frac{\tilde\theta_i z_{i,1}^{\mathrm{T}}z_{i,1}S_{i,1}^{\mathrm{T}}S_{i,1}}{2l_{i,1}^2}-\frac{\tilde\theta_i z_{i,2}^{\mathrm{T}}z_{i,2}S_{i,2}^{\mathrm{T}}S_{i,2}}{2l_{i,2}^2}-V_{i,3}+\\&\frac12\theta_i^2+2^{\frac{1+\alpha}{2}}\frac{\gamma}{T_\rho}(\mathrm{sgn}^{\alpha}(\hat\theta_i))\tilde\theta_i+\\&2^{\frac{1+\beta}{2}}\frac{\gamma}{T_\rho}(\mathrm{sgn}^{\beta}(\hat\theta_i))\tilde\theta_i\end{aligned} \tag{53}$$

For the fifth item of Eq. (53), we have

$$\begin{aligned}2^{\frac{1+\alpha}{2}}\frac{\gamma}{T_\rho}(\mathrm{sgn}^{\alpha}(\hat\theta_i))\tilde\theta_i=&2^{\frac{1+\alpha}{2}}\frac{\gamma}{T_\rho}(\mathrm{sgn}^{\alpha}(\hat\theta_i))\theta_i-\\&2^{\frac{1+\alpha}{2}}\frac{\gamma}{T_\rho}(\mathrm{sgn}^{\alpha}(\hat\theta_i))\hat\theta_i\end{aligned} \tag{54}$$

According to Lemma 2, taking $a=1+\alpha$, $b=1+1/\alpha$, and $\varepsilon=b^{-\frac{1}{b}}$, we have

$$2(\mathrm{sgn}^{\alpha}(\hat\theta_i))\theta_i\leqslant\frac{\alpha^{\alpha}|2\theta_i|^{1+\alpha}}{(1+\alpha)^{1+\alpha}}+|\hat\theta_i|^{1+\alpha} \tag{55}$$

Combining Eq. (54) and Formula (55), one gets

$$\begin{aligned}&2\frac{2^{\frac{\alpha-1}{2}}\gamma}{T_\rho}(\mathrm{sgn}^{\alpha}(\hat\theta_i))\tilde\theta_i\leqslant\\&2^{\frac{\alpha-1}{2}}\frac{\gamma}{T_\rho}|\hat\theta_i|^{1+\alpha}+2^{\frac{\alpha-1}{2}}\frac{\gamma}{T_\rho}\frac{\alpha^{\alpha}|2\theta_i|^{1+\alpha}}{(1+\alpha)^{1+\alpha}}-\\&2\frac{2^{\frac{\alpha-1}{2}}\gamma}{T_\rho}(\mathrm{sgn}^{\alpha}(\hat\theta_i))\hat\theta_i=\\&2^{\frac{\alpha-1}{2}}\frac{\gamma}{T_\rho}\left(\frac{\alpha^{\alpha}|2\theta_i|^{1+\alpha}}{(1+\alpha)^{1+\alpha}}+|\theta_i|^{1+\alpha}\right)-\\&2^{\frac{\alpha-1}{2}}\frac{\gamma}{T_\rho}\left(|\theta_i|^{1+\alpha}+|\hat\theta_i|^{1+\alpha}\right)\end{aligned} \tag{56}$$

Let $\mu_1=|\theta_i|$, $\mu_2=|\hat\theta_i|$, $d=1+\alpha$, and $Q=2$. It thus follows from Lemma 3 and $|\theta_i|+|\hat\theta_i|\geqslant\theta_i-\hat\theta_i$ that

$$\begin{aligned}&-2^{\alpha}\left(|\theta_i|^{1+\alpha}+|\hat\theta_i|^{1+\alpha}\right)\leqslant\\&-2^{\alpha}\left[2^{1-(1+\alpha)}(|\theta_i|+|\hat\theta_i|)^{1+\alpha}\right]=\\&-(|\theta_i|+|\hat\theta_i|)^{1+\alpha}\leqslant\\&-(\theta_i-\hat\theta_i)^{1+\alpha}=\\&-(\tilde\theta_i^2)^{\frac{1+\alpha}{2}}\end{aligned} \tag{57}$$

From the second item of Formula (56), one has

$$\begin{aligned}&-\left(\frac12\right)^{\frac{1+\alpha}{2}}\frac{2^{\alpha}\gamma}{T_\rho}\left(|\theta_i|^{1+\alpha}+|\hat\theta_i|^{1+\alpha}\right)\leqslant\\&-\left(\frac12\right)^{\frac{1+\alpha}{2}}\frac{\gamma}{T_\rho}(\tilde\theta_i^2)^{\frac{1+\alpha}{2}}=\\&-\frac{\gamma}{T_\rho}V_{i,3}^{\frac{1+\alpha}{2}}\end{aligned} \tag{58}$$

Likewise, for the final item in Eq. (53), one derives

$$\begin{aligned}2^{\frac{1+\beta}{2}}\frac{\gamma}{T_\rho}(\mathrm{sgn}^{\beta}(\hat\theta_i))\tilde\theta_i\leqslant&2^{\frac{\beta-1}{2}}\frac{\gamma}{T_\rho}\left(\frac{\beta^{\beta}|2\theta_i|^{1+\beta}}{(1+\beta)^{1+\beta}}+|\theta_i|^{1+\beta}\right)-\\&2^{\frac{\beta-1}{2}}\frac{\gamma}{T_\rho}\left(|\theta_i|^{1+\beta}+|\hat\theta_i|^{1+\beta}\right)\leqslant\\&2^{\frac{\beta-1}{2}}\frac{\gamma}{T_\rho}\left(\frac{\beta^{\beta}|2\theta_i|^{1+\beta}}{(1+\beta)^{1+\beta}}+|\theta_i|^{1+\beta}\right)-\\&\frac{\gamma}{T_\rho}V_{i,3}^{\frac{1+\beta}{2}}\end{aligned} \tag{59}$$

Substituting Formulas (54)–(59) into Eq. (53) yields

$$\begin{aligned}\dot V_{i,3}\leqslant&-\frac{\gamma}{T_\rho}V_{i,3}^{\frac{1+\alpha}{2}}-\frac{\gamma}{T_\rho}V_{i,3}^{\frac{1+\beta}{2}}-V_{i,3}-\\&\frac{\tilde\theta_i z_{i,1}^{\mathrm{T}}z_{i,1}S_{i,1}^{\mathrm{T}}S_{i,1}}{2l_{i,1}^2}-\frac{\tilde\theta_i z_{i,2}^{\mathrm{T}}z_{i,2}S_{i,2}^{\mathrm{T}}S_{i,2}}{2l_{i,2}^2}+\varDelta_3\end{aligned} \tag{60}$$

where

$$\varDelta_3=\frac{1}{2}\theta_i^2+2^{\frac{\alpha-1}{2}}\frac{\gamma}{T_\rho}\left(\frac{\alpha^\alpha|2\theta_i|^{1+\alpha}}{(1+\alpha)^{1+\alpha}}+|\theta_i|^{1+\alpha}\right)+ 2^{\frac{\beta-1}{2}}\frac{\gamma}{T_\rho}\left(\frac{\beta^\beta|2\theta_i|^{1+\beta}}{(1+\beta)^{1+\beta}}+|\theta_i|^{1+\beta}\right).$$

Algorithm 1 outlines the procedure to elucidate the controller design.

Algorithm 1 Procedure of controller design

Initialization:

Initialize $z_{i,1}(0)$ and $\hat{\theta}_i(0)$, $i=1,2,...,N$

Parameter selection:

Predefined time $T_\rho \geqslant T_o$

Given directed augmented network $\bar{G}$

Determine the number of following agents N

Choose the strength of feedback gain $\sigma>0$

Choose designed parameters $l_{i,1}$, $l_{i,2}$, n_1, n_2, and D

Specify constants $0<\alpha<1$ and $\beta>1$

Parameter computation:

$\frac{1-\alpha}{\beta-\alpha}\rightarrow m_1$

$\frac{\beta-1}{\beta-\alpha}\rightarrow m_2$

$\frac{\varGamma(m_1)\varGamma(m_2)}{\beta-\alpha}3^{\frac{(\beta-1)(1-\alpha)}{2(\beta-\alpha)}}\rightarrow\gamma$

Parameter adaptive law:

Equation (51)$\rightarrow \hat{\theta}_i(t)$

Virtual controllers:

Equation (27) $\rightarrow \alpha_{i,1}$

Equation (46)$\rightarrow \alpha_{i,2}$

Controller update:

Equation (40)$\rightarrow \tau_i(t)$

IV. STABILITY ANALYSIS

Theorem 1 For the robotic MASs in Eq. (2), with the help of Assumption 1 and Lemmas 1–7, suppose that the virtual controllers in Eqs. (27) and (46), the parameter adaptive law in Eq. (51), and the switching thresholds ETC mechanism in Eq. (41) are designed. Then, the proposed approach ensures that all signals have boundaries and the tracking errors converge to a small neighborhood around the origin within the predefined time T_ρ. Besides, the Zeno phenomenon is avoided effectively.

Proof Differentiating V gives

$$\dot{V}=\dot{V}_{i,1}+\dot{V}_{i,2}+\dot{V}_{i,3} \tag{61}$$

Combining Formulas (32), (49), and (60) yields

$$\dot{V}\leqslant-\sigma V_{i,1}-\sigma V_{i,2}-V_{i,3}- \frac{\gamma}{T_\rho}V_{i,1}^{\frac{1+\alpha}{2}}-\frac{\gamma}{T_\rho}V_{i,1}^{\frac{1+\beta}{2}}-\frac{\gamma}{T_\rho}V_{i,2}^{\frac{1+\alpha}{2}}- \frac{\gamma}{T_\rho}V_{i,2}^{\frac{1+\beta}{2}}-\frac{\gamma}{T_\rho}V_{i,3}^{\frac{1+\alpha}{2}}-\frac{\gamma}{T_\rho}V_{i,3}^{\frac{1+\beta}{2}}+\varDelta \tag{62}$$

where $\varDelta=\varDelta_1+\varDelta_2+\varDelta_3$.

Therefore, it follows from Formula (62) through Lemma 3 that

$$\dot{V}\leqslant-\frac{\gamma}{T_\rho}\left(V^{\frac{1+\alpha}{2}}+3^{\frac{1-\beta}{2}}V^{\frac{1+\beta}{2}}\right)-\zeta V+\varDelta \tag{63}$$

where $\zeta=\min\{\sigma,1\}$. According to Lemma 7, we have $m_1=(1-\alpha)/(\beta-\alpha)$, $m_2=(\beta-1)/(\beta-\alpha)$, and $\gamma=((\varGamma(m_1)\varGamma(m_2))/(\beta-\alpha))3^{\frac{(\beta-1)(1-\alpha)}{2(\beta-\alpha)}}$. Therefore, the robotic MASs in Eq. (2) achieve SGUPTB leader-following consensus. ■

Remark 2 From Formula (63), let $\varOmega=\{x\in\mathbb{R}^n|V(x)\leqslant\varDelta/\zeta\}$. Since $x\notin\varOmega$, it can be obtained that $V(x)>\varDelta/\zeta$. The following inequality holds

$$\dot{V}\leqslant-\frac{\gamma}{T_\rho}\left(V^{\frac{1+\alpha}{2}}+3^{\frac{1-\beta}{2}}V^{\frac{1+\beta}{2}}\right) \tag{64}$$

From Formula (64), the equilibrium point $x=0$ is strongly predefined-time stable. Thus, there are a tunable bounded constant $\varUpsilon>0$, a finite bound $\varepsilon_\rho\overset{\Delta}{=}\varepsilon_\rho>0$, and a predefined time T_ρ, such that solution $x=x(t,x_0)$ satisfies that $\forall t\geqslant T_\rho$ and $\forall x_0\in\{x\in\mathbb{R}^n|\,||x||\leqslant\eta,\forall\eta\in(0,\varUpsilon)\}$.

$$||x(t,x_0)||\leqslant\varepsilon_\rho \tag{65}$$

where T_ρ and ε_ρ are independent of the initial state and system parameters. It follows that the equilibrium point is SGUPTB stable and $\lim_{t\to\infty}||x(t,x_0)||=0$.

If $x\in\varOmega$, then Formula (63) holds. Once x reaches the boundary of $\varOmega$, its trajectory will not leave the set $\varOmega$, as $\dot{V}\leqslant 0$.

From the preceding discussions, it follows that $\forall t\geqslant T_\rho$ and $x\in\varOmega$. Let $\delta_1\in(0,+\infty)$ be a sufficiently large constant and define $\varOmega_1=\{x\in\varOmega|\,||x||<\delta_1\}$. The set $\varOmega_1\in\varOmega$ is nonempty, closed, and bounded, indicating a bounded constant $\varepsilon_\rho>0$, such that $||x||\leqslant\varepsilon_\rho$ for all $x\in\varOmega_1$. Let $\varpi\in(0,+\infty)$, setting $\varUpsilon=\min\{\varpi\ \ |\,||x||\leqslant\varpi,\forall x\in\varOmega_1\}$, Formula (65) holds, confirming that the equilibrium point is SGUPTB stable. Thus, the boundedness of $x_{i,1}$, $x_{i,2}$, $z_{i,1}$, $z_{i,2}$, $\hat{\theta}_i$, $\alpha_{i,1}$, and $\alpha_{i,2}$ can be concluded.

Remark 3 The Zeno behavior is fully considered. For $\forall k\in\mathbb{Z}^+$, define $\bar{t}$ with $t_{k+1}-t_k>\bar{t}$. From the event-triggered controller in Eq. (41), since all closed-loop signals have been proved to be bounded, we can get a constant $\sigma>0$, such that $|\dot{e}_i(t)|\leqslant\sigma$. Furthermore, $e_i(t_k)=0$ and $\lim_{t\to t_{k+1}}e_i(t)=\rho|\tau_i(t)|+n_1$ or $\lim_{t\to t_{k+1}}e_i(t)=n_2$. According to the above description, we can get that the lower bound of $\bar{t}$ must satisfy $\bar{t}\geqslant\min\{(\rho|\tau_i(t)|+n_1)/\sigma,n_2/\sigma\}$.

According to Lemma 7, we can know that V converts in a range defined as $\varOmega=\{V(x)|V(x)<\varDelta/\zeta\}$ in the predefined time.

By modifying the aforementioned design parameters, the consensus tracking control protocol can ensure that the tracking errors converge to a small neighborhood of the origin. We can further obtain

$$\lim_{t\to T_\rho}||y-\bar{y}_{\rm d}||\leqslant\upsilon \tag{66}$$

Due to the definition of V, one has

$$||z_1||^2\leqslant\frac{2\varDelta}{\zeta} \tag{67}$$

By adjusting the parameters $l_{i,1}$, $l_{i,2}$, and σ, we can obtain

$$\frac{\Delta}{\zeta} \leqslant \frac{\upsilon^2}{2}(\sigma(L+B))^2 \tag{68}$$

Based on Formula (68) and Lemma 1, we can obtain Formula (66) for any $\upsilon > 0$.

V. SIMULATION STUDY

To prove the efficiency of our developed control strategy in practical applications, the two-link robotic MASs are researched for the simulation. The plant dynamics of the i-th robot is represented as

$$M_i(q_i)\ddot{q}_i + C_i(q_i,\dot{q}_i)\dot{q}_i + G_i(q_i) + f_{\text{dis}}(t) = \tau_i \tag{69}$$

Let $x_{i,1} = q_i$ and $x_{i,2} = \dot{q}_i$, where $q_i = [q_{i,1}, q_{i,2}]^{\mathrm{T}} \in \mathbb{R}^2$. We transform Eq. (69) with new state variables. Then, the robot dynamics can be shown as

$$\begin{cases} \dot{x}_{i,1} = x_{i,2}, \\ \dot{x}_{i,2} = M_i^{-1}(\tau_i - C_i x_{i,2} - G_i - f_{\text{dis}}) \end{cases} \tag{70}$$

Definitions $M_i(x_{i,1})$, $C_i(x_{i,1}, x_{i,2})$, and $G_i(x_{i,1})$ can be expressed as

$$M_i(x_{i,1}) = \begin{bmatrix} M_{11} & M_{12} \\ M_{21} & M_{22} \end{bmatrix} \tag{71}$$

$$C_i(x_{i,1}, x_{i,2}) = \begin{bmatrix} C_{11} & C_{12} \\ C_{21} & 0 \end{bmatrix} \tag{72}$$

$$G_i(x_{i,1}) = \begin{bmatrix} G_{11} \\ G_{21} \end{bmatrix} \tag{73}$$

where

$$\begin{aligned} &M_{11} = m_1 d_1^2 + m_2\left(d_1^2 + d_2^2 + 2d_1 d_2 \cos q_{i,2}\right), \\ &M_{12} = M_{21} = m_2\left(d_2^2 + d_1 d_2 \cos q_{i,2}\right), \\ &M_{22} = m_2 d_2^2, \\ &C_{11} = -m_2 d_1 d_2 \dot{q}_{i,2} \sin q_{i,2}, \\ &C_{12} = -m_2 d_1 d_2 (\dot{q}_{i,1} + \dot{q}_{i,2}) \sin q_{i,2}, \\ &C_{21} = -m_2 d_1 d_2 \dot{q}_{i,1} \sin q_{i,2}, \\ &G_{11} = (m_1 d_2 + m_2 d_1) g \cos q_{i,1} + m_2 d_2 g \cos(q_{i,1} + q_{i,2}), \\ &G_{21} = m_2 d_2 g \cos(q_{i,1} + q_{i,2}) \end{aligned} \tag{74}$$

The initial position of the robot is given as $q_0 = [0,0]$. The desired trajectory is chosen as $y_d = [\sin(0.5\pi t), \sin(0.5\pi t)]$. The system parameters for the two-link robot manipulator system are given in Table 1.

Table 1 Simulation parameter.

Parameter	Description	Value	Unit
m_1	Mass of link 1	1	kg
m_2	Mass of link 2	1	kg
d_1	Length of link 1	0.8	m
d_2	Length of link 2	0.7	m
g	Gravitational acceleration	9.8	m/s^2
T_ρ	Predefined time	0.2	s
σ	Feedback gain	1	—
$l_{i,1}$ and $l_{i,2}$	Designed parameter	1 and 1	—
α and β	Designed parameter	0.5 and 3.0	—
n_1, n_2, and D	Designed parameter	0.5, 0.7, and 10	—

The adjacency matrix represents the weighting relationships between agents, and the Laplacian matrix of the system is defined by graph theory. They can be expressed as $A = \begin{bmatrix} 0 & 0 & 0 \\ 1 & 0 & 0 \\ 2 & 0 & 0 \end{bmatrix}$ and $L = \begin{bmatrix} 0 & 0 & 0 \\ -1 & 1 & 0 \\ -2 & 0 & 2 \end{bmatrix}$. Figure 1 shows the robotic MASs communication topology. Diagram of a two-link robotic manipulator is shown in Fig. 2. Figures 3–5 show that the output trajectories of all followers q_i converge to the leader y_d within $T_\rho = 0.2$. Figure 6 shows that the tracking errors among the leader and three followers converge to the small neighborhood range of the origin within $T_\rho = 0.2$. Figure 7 represents that the adaptive parameters of each follower are bounded for $T_\rho = 0.2$, and the control inputs τ_i under event-triggered mechanism are shown in Figs. 8–10. The inter-times trajectories of τ_i are shown in Figs. 11–13,

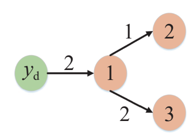

Figure 1 MASs communication topology.

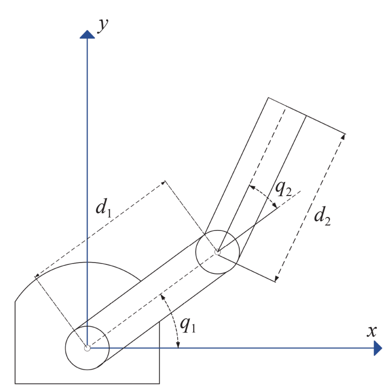

Figure 2 Diagram of a two-link robotic manipulator.

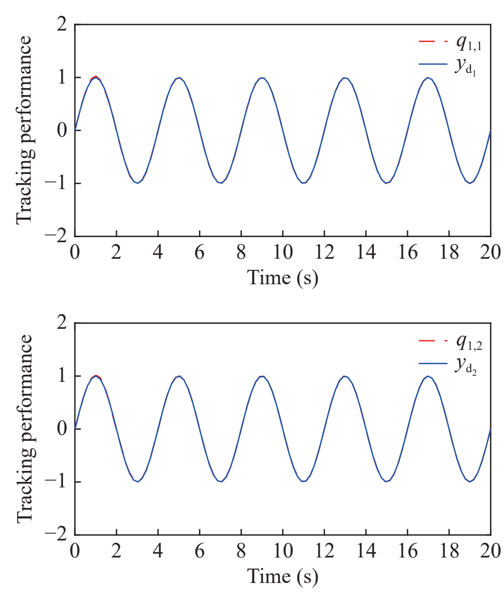

Figure 3 Trajectory of agent one and the leader.

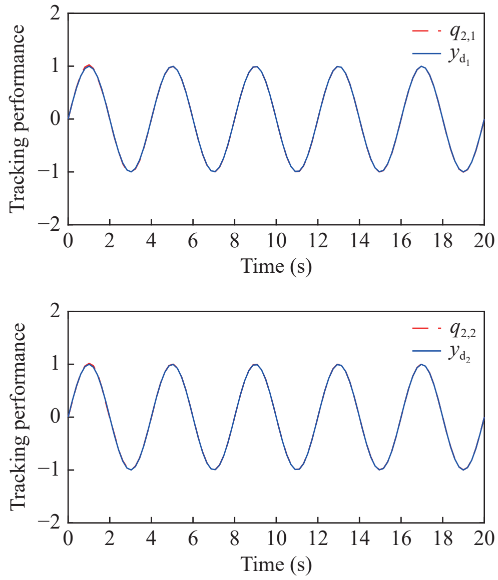

Figure 4 Trajectory of agent two and the leader.

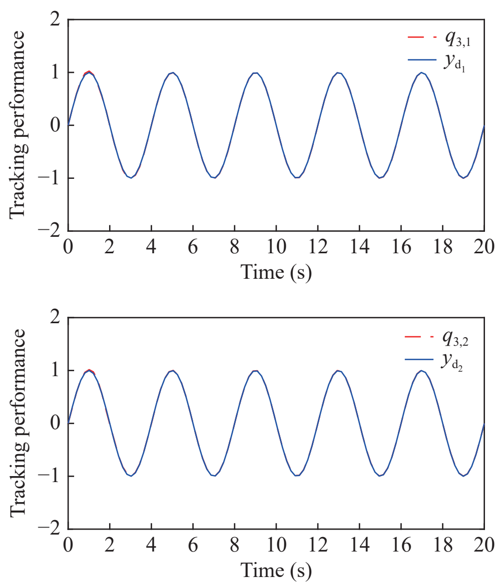

Figure 5 Trajectory of agent three and the leader.

which demonstrate the effectiveness of the event-triggered mechanism.

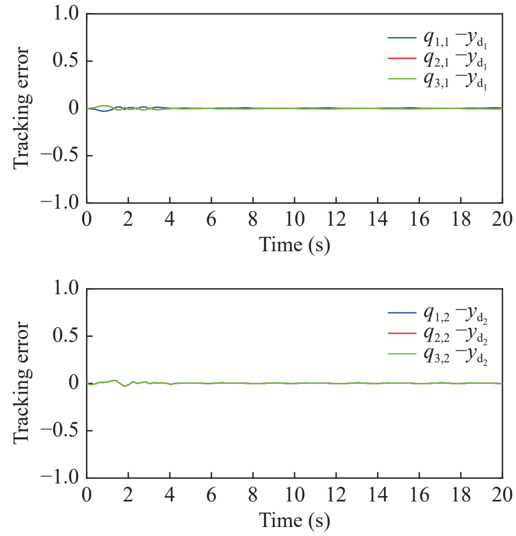

Figure 6 Trajectory of the error.

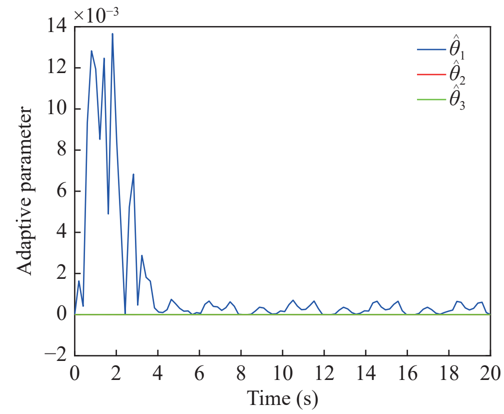

Figure 7 Adaptive parameter.

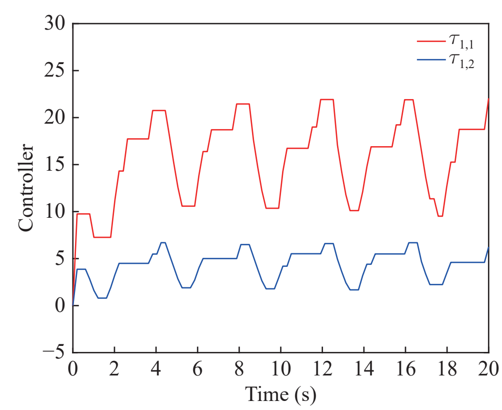

Figure 8 Control input of agent one.

VI. CONCLUSION

This article proposes an adaptive predefined-time event-triggered consensus tracking control strategy for the robotic MASs, which enables each robotic manipulator to track the ideal signal of the leader. Moreover, the switching thresholds ETC mechanism saves network resources and guarantees that all signals have boundaries without the Zeno phenomenon in the closed-loop system. The RBFNNs are employed to address unknown disturbance term $f_{\text{dis}}(t)$, which provides the control mechanism proposed with a certain level of fault tolerance. Because of the fact that the robotic MASs may be running on unsecured networks, the consensus tracking control problem of the robotic MASs based on the predefined-time control strategy under the denial-of-service attacks will be taken into consideration in future studies.

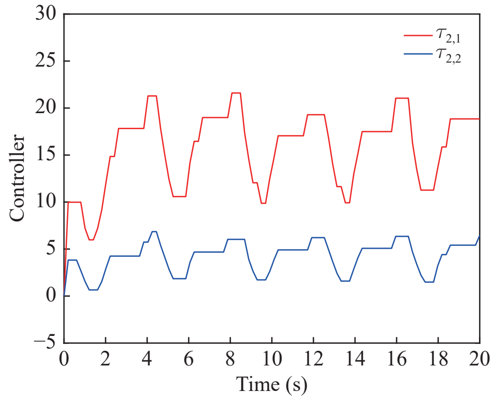

Figure 9 Control input of agent two.

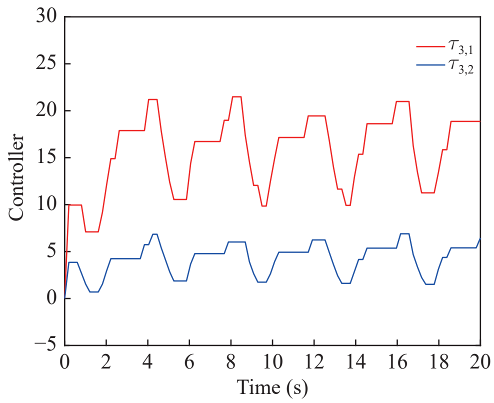

Figure 10 Control input of agent three.

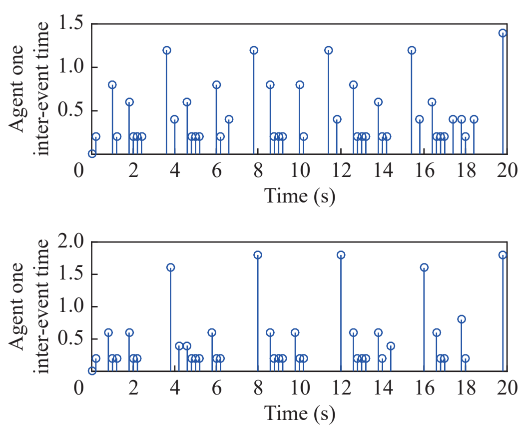

Figure 11 Inter-event time of agent one.

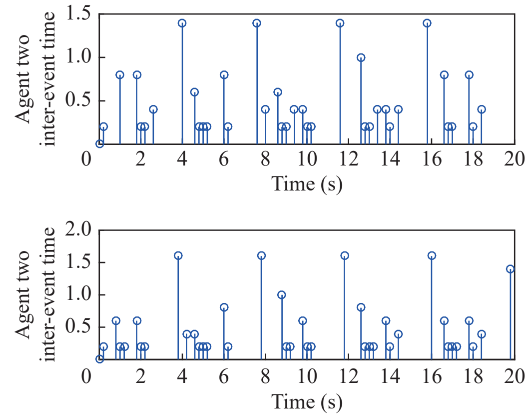

Figure 12 Inter-event time of agent two.

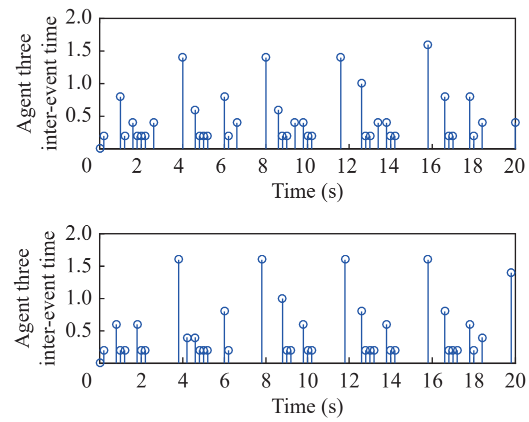

Figure 13 Inter-event time of agent three.

REFERENCES

[1] B. Cai, C. Sheng, C. Gao, Y. Liu, M. Shi, Z. Liu, Q. Feng, and G. Liu, Artificial intelligence enhanced reliability assessment methodology with small samples, *IEEE Trans. Neural Netw. Learn. Syst.*, 2023, 34(9), 6578–6590.

[2] S. U. Jan, Y. D. Lee, and I. S. Koo, A distributed sensor-fault detection and diagnosis framework using machine learning, *Inf. Sci.*, 2021, 547, 777–796.

[3] Y. Xu, Y. Zhang, and J.-F. Zhang, Singularity-free adaptive control of MIMO discrete-time nonlinear systems with general vector relative degrees, *Automatica*, 2023, 153, 111054.

[4] S. He, X. Liu, P. Lu, C. Du, and H. Liu, Distributed finite-time consensus algorithm for multiagent systems via aperiodically intermittent protocol, *IEEE Trans. Circuits Syst. II: Express Briefs*, 2022, 69(7), 3229–3233.

[5] W. Sun, S. Su, Y. Wu, J. Xia, and V. Nguyen, Adaptive fuzzy control with high-order barrier Lyapunov functions for high-order uncertain nonlinear systems with full-state constraints, *IEEE Trans. Cybern.*, 2020, 50(8), 3424–3432.

[6] Y. Zhang, J. Sun, H. Li, and W. He, Event-triggered adaptive bipartite containment control for stochastic multiagent systems, *IEEE Trans. Syst., Man, Cybern.: Syst.*, 2022, 52(9), 5843–5852.

[7] J. Zhang, Y. Fu, and J. Fu, Adaptive finite-time optimal formation control for second-order nonlinear multiagent systems, *IEEE Trans. Syst., Man, Cybern.: Syst.*, 2023, 53(10), 6132–6144.

[8] D. Bao, X. Liang, S.-S. Ge, and B. Hou, Adaptive neural trajectory tracking control for *n*-DOF robotic manipulators with state constraints, *IEEE Trans. Ind. Inf.*, 2023, 19(7), 8039–8048.

[9] H. Ma, Q. Zhou, H. Li, and R. Lu, Adaptive prescribed performance control of a flexible-joint robotic manipulator with dynamic uncertainties, *IEEE Trans. Cybern.*, 2022, 52(12), 12905–12915.

[10] X. You, C. Hua, K. Li, and X. Jia, Fixed-time leader-following consensus for high-order time-varying nonlinear multiagent systems, *IEEE Trans. Autom. Control*, 2020, 65(12), 5510–5516.

[11] A. N. Nekhoroshikh, D. Efimov, A. Polyakov, W. Perruquetti, and I. B. Furtat, Hyperexponential and fixed-time stability of time-delay systems: Lyapunov-Razumikhin method, *IEEE Trans. Autom. Control*, 2023, 68(3), 1862–1869.

[12] J. Ma, J. Wang, S. Fei, and Y. Liu, Global fixed-time control for nonlinear systems with unknown control coefficients and dead-zone input, *IEEE Trans. Circuits Syst. II: Express Briefs*, 2022, 69(2), 594–598.

[13] Z. Shang, Y. Jiang, B. Niu, G. Zong, X. Zhao, and H. Li, Adaptive finite-time consensus tracking control for nonlinear multi-agent systems: An improved tan-type nonlinear mapping function method, *IEEE Trans. Autom. Sci. Eng.*, 2024, 21(4), 5434–5444.

[14] X. Fang, H. Fan, W. Wang, L. Liu, B. Wang, and Z. Cheng, Adaptive finite-time fault-tolerant control of uncertain systems with input

saturation, *IEEE Trans. Syst., Man, Cybern.: Syst.*, 2023, 53(1), 165–177.

[15] Q. Meng, Q. Ma, and Y. Shi, Adaptive fixed-time stabilization for a class of uncertain nonlinear systems, *IEEE Trans. Autom. Control*, 2023, 68(11), 6929–6936.

[16] L. Cheng, F. Tang, X. Shi, X. Chen, and J. Qiu, Finite-time and fixed-time synchronization of delayed memristive neural networks via adaptive aperiodically intermittent adjustment strategy, *IEEE Trans. Neural Netw. Learning Syst.*, 2023, 34(11), 8516–8530.

[17] Q. Xiao, H. Liu, and Y. Wang, An improved finite-time and fixed-time stable synchronization of coupled discontinuous neural networks, *IEEE Trans. Neural Netw. Learning Syst.*, 2023, 34(7), 3516–3526.

[18] Z. Cai, L. Huang, and Z. Wang, Finite-/fixed-time stability of nonautonomous functional differential inclusion: Lyapunov approach involving indefinite derivative, *IEEE Trans. Neural Netw. Learning Syst.*, 2022, 33(11), 6763–6774.

[19] Y. Pan, W. Ji, H.-K. Lam, and L. Cao, An improved predefined-time adaptive neural control approach for nonlinear multiagent systems, *IEEE Trans. Autom. Sci. Eng.*, 2024, 21(4), 6311–6320.

[20] F. Jia, J. Huang, and X. He, Predefined-time fault-tolerant control for a class of nonlinear systems with actuator faults and unknown mismatched disturbances, *IEEE Trans. Autom. Sci. Eng.*, 2024, 21(3), 3801–3815.

[21] F. Li and Y. Liu, Event-triggered stabilization for continuous-time stochastic systems, *IEEE Trans. Autom. Control*, 2020, 65(10), 4031–4046.

[22] S. Diao, W. Sun, S. Su, and J. Xia, Adaptive fuzzy event-triggered control for single-link flexible-joint robots with actuator failures, *IEEE Trans. Cybern.*, 2022, 52(8), 7231–7241.

[23] B. Liang, S. Zheng, C. K. Ahn, and F. Liu, Adaptive fuzzy control for fractional-order interconnected systems with unknown control directions, *IEEE Trans. Fuzzy Syst.*, 2022, 30(1), 75–87.

[24] J. Qiu, T. Wang, K. Sun, I. J. Rudas, and H. Gao, Disturbance observer-based adaptive fuzzy control for strict-feedback nonlinear systems with finite-time prescribed performance, *IEEE Trans. Fuzzy Syst.*, 2022, 30(4), 1175–1184.

[25] Y. Sheng, Z. Zeng, and T. Huang, Global stability of bidirectional associative memory neural networks with multiple time-varying delays, *IEEE Trans. Cybern.*, 2022, 52(6), 4095–4104.

[26] C. Yan, J. Xia, J. H. Park, J. Feng, and X. Xie, Fully actuated system approach-based dynamic event-triggered control with guaranteed transient performance of flexible-joint robot: Experiment, *IEEE Trans. Circuits Syst. II Exp. Briefs*, 2024, 71(8), 3775–3779.

[27] Y. Zhang, Y. Lei, T. Zhang, R. Song, Y. Li, and F. Du, Robust command-filtered control with prescribed performance for flexible-joint robots, *IEEE Trans. Instrum. Meas.*, 2023, 72, 1–13.

[28] E. Kang, H. Qiao, Z. Chen, and J. Gao, Tracking of uncertain robotic manipulators using event-triggered model predictive control with learning terminal cost, *IEEE Trans. Autom. Sci. Eng.*, 2022, 19(4), 2801–2815.

[29] S. Kang, P.-X. Liu, and H. Wang, Adaptive fuzzy finite-time command filtering control for flexible-joint robot systems against multiple actuator constraints, *IEEE Trans. Circuits Syst. II: Express Briefs*, 2023, 70(12), 4554–4558.

[30] S. Liu, H. Wang, T. Li, and K. Xu, Adaptive neural fixed-time control for uncertain nonlinear systems, *IEEE Trans. Circuits Syst. II: Express Briefs*, 2024, 71(2), 637–641.

[31] H. Zhang, F. L. Lewis, and Z. Qu, Lyapunov, adaptive, and optimal design techniques for cooperative systems on directed communication graphs, *IEEE Trans. Ind. Electron.*, 2012, 59(7), 3026–3041.

[32] H. Wang and Q. Zhu, Adaptive output feedback control of stochastic nonholonomic systems with nonlinear parameterization, *Automatica*, 2018, 98, 247–255.

[33] B. Niu, J. Sui, X. Zhao, D. Wang, X. Zhao, and Y. Niu, Adaptive fuzzy practical predefined-time bipartite consensus tracking control for heterogeneous nonlinear MASs with actuator faults, *IEEE Trans. Fuzzy Syst.*, 2024, 32(5), 3071–3083.

[34] Y. Shang, B. Chen, and C. Lin, Consensus tracking control for distributed nonlinear multiagent systems via adaptive neural backstepping approach, *IEEE Trans. Syst. Man Cybern. Syst.*, 2020, 50(7), 2436–2444.

[35] X.-A. Wang, G.-J. Zhang, B. Niu, D. Wang, and X.-M. Wang, Event-triggered-based consensus neural network tracking control for nonlinear pure-feedback multiagent systems with delayed full-state constraints, *IEEE Trans. Autom. Sci. Eng.*, 2024, 21(4), 7390–7400.

[36] B. Mao, X. Wu, H. Liu, Y. Xu, and J. Lü, Adaptive fuzzy tracking control with global prescribed-time prescribed performance for uncertain strict-feedback nonlinear systems, *IEEE Trans. Cybern.*, 2024, 54(9), 5217–5230.

[37] B. Mao, X. Wu, J. Lü, and G. Chen, Predefined-time bounded consensus of multiagent systems with unknown nonlinearity via distributed adaptive fuzzy control, *IEEE Trans. Cybern.*, 2023, 53(4), 2622–2635.

Tengying Yan received the BS degree from Shandong Jiaotong University, China, in 2023. He is currently pursuing the MS degree at Shandong Normal University, China. His research interests include adaptive control, constraint control, and nonlinear MASs.

Xinliang Zhao received the BS degree from Shandong Management University, China, in 2022. He is currently pursuing the MS degree at Shandong Normal University, China. His research interests include adaptive control, intelligent control, and nonlinear MASs.

Yuhan Zhang received the BS degree from Weifang University, China, in 2022. She is currently pursuing the MS degree at Shandong Normal University, China. Her research interests include adaptive control, nonlinear MASs, and formation control.

Yulong Ji received the BS degree from Liaocheng University, China, in 2022. He is currently pursuing the MS degree at Shandong Normal University, China. His research interests include adaptive control, nonlinear MASs, and formation control.

Ben Niu received the PhD degree in control theory and control engineering from Northeastern University, Shenyang, China, in 2013. He is currently a professor at School of Information Science and Engineering, Shandong Normal University, Jinan, China. His research interests include switched systems, stochastic systems, adaptive control, intelligent control, and their applications.